Asian Journal of Chemistry; Vol. 27, No. 7 (2015), 2608-2618

ASIAN JOURNAL OF CHEMISTRY

http://dx.doi.org/10.14233/ajchem.2015.18543

# Influence of Heat Treatment and Dispersing Agent Addition on Hydroxyapatite Powder Properties and its Suspension Characteristics

Y.M.Z. AHMED[1,*], S.M. EL-SHEIKH[2] and Z.I. ZAKI[1]

[1]Ceramic and Refractory Materials Division, Central Metallurgical Research and Development Institute, P.O. Box 87, Helwan 11421, Egypt
[2]Nano-Structured Materials Division, Central Metallurgical Research and Development Institute, P.O. Box 87, Helwan 11421, Egypt

*Corresponding author: Fax: +20 2 5010639; Tel: +20 2 5010642; E-mail: ahmedymz@hotmail.com

*Received*: 1 August 2014; *Accepted*: 10 December 2014; *Published online*: 30 March 2015; AJC-17089

Colloidal processing route is considered as a potential way of successfully fabricating a homogeneous and complex shape ceramic body. In this regards, preparation of a well dispersed ceramic suspension is a vital in deciding the suitability of applying this processing route for ceramic green body fabrication. Controlling the physical properties of hydroxyapatite powder through the calcination process would enhance the particle properties in terms of particle size, its distribution and surface area. It was found that hydroxyapatite powder calcined at 1100 °C possesses physical and chemical properties suitable for colloidal processing route. Also the utilizing of calcined powder at 1100 °C with 0.3 wt. % sodium polyacrylate dispersant proved to be beneficial in producing a low viscosity and high turbidity suspensions.

**Keywords: Hydroxyapatite, Heat treatment, Particle size, Zeta potential, Viscosity, Turbidity.**

## INTRODUCTION

Hydroxyapatite (HA) and related calcium phosphate (CP) materials have been widely used as implant materials for many years due to their close similarity in composition and high biocompatibility with natural bone[1-4]. However, the low mechanical reliability of the sintered hydroxyapatite body limiting their uses[5,6]. Recently, a significant effort to overcome this problem was taken place in finding a suitable fabrication route for hydroxyapatite ceramics other than the traditional one (like dry powder consolidation method)[7]. The colloidal processing route could be promising in this regards. The colloidal approach has the potential for eliminating detrimental heterogeneity, avoiding their reintroduction during the successive processing steps and obtaining pieces with intricate shapes similar to human bones[8]. The most important and vital step in the successful utilizing this route for ceramic fabrication, is the preparation of highly homogeneous and well dispersed ceramic suspension prior to casting. This could be accomplished *via* both (1) controlling the physical properties of the hydroxyapatite powder in terms of particle size, particle size distribution, particle surface charge and surface area, (2) selecting an appropriate dispersant in terms of type and amount. It is well known that, in order to produce well stabilized colloidal ceramic suspensions, it is necessary to use powders with low surface area, because powders with high surface area tend to form undesirable agglomerates[9]. These agglomerates are thought to be "soft agglomerate" formed by vander Waals force and can be easily broken by mixing[10]. Such agglomerates are known to be difficult to disperse due to their surface charge state[11] and producing of very small particle size upon mixing. On the other hand powders with the extremely low surface area have higher density and grain size could be settled out resulting in density heterogeneity in the green body. Therefore, a compromise between these aspects must be acheived. In addition, to improve the various properties of the final hydroxyapatite sintered sample, well stabilized suspensions with a high hydroxyapatite concentration should be prepared. The nature of the surface of hydroxyapatite particles plays a key role in the rheological properties of the formed suspensions[12].

One way in monitoring the physical and chemical properties of hydroxyapatite powder is through calcination process. It was earlier mentioned that the calcination of the hydroxyapatite powder is affected by a large degree of its physical properties[13-18]. They explored in their work the influence of different calcination temperatures on some physical properties of the hydroxyapatite powder in the temperature range of 400 to maximum 1000 °C. They did not elaborate in their investigation the relation between these changes (physical and chemical properties of hydroxyapatite) with the formation of stabilized suspensions.

Herein different calcination temperatures starting from 800 to 1100 °C were applied. The effect of these calcination temperatures on the physical and chemical properties of the

hydroxyapatite powder was thoroughly investigated. The correlation between the changes in the physico-chemical properties of hydroxyapatite powder for preparing a well stabilized hydroxyapatite suspension was carried out. Besides, the influence of adding different types and amounts of dispersant on the viscosity as well as turbidity of hydroxyapatite suspension produced from hydroxyapatite powder calcined at various temperatures was studied.

**Materials and procedures:** Hydroxyapatite powder used in this project was delivered from Riedel-de Haen Co. (Seelze, Germany). In order to study the deflocculation ability of the hydroxyapatite powder, two types of dispersing agents were applied in this investigation. The first is Acumar 9400 which is a water-soluble sodium salt polymer used to disperse and stabilize high-solids mineral slurries. It is an anionic dispersant of sodium polyacrylate polymer (SPA) of solid content 41-43 wt. % with a molecular weight of 3000-4000. Other dispersant is poly acrylic acid dispersant. Polyacrylic acid (PAA) is a polymer dispersant. It can be used in situations of alkaline and high concentration without scale sediment. The solid content of this type of dispersant is 40 wt. %.

## EXPERIMENTAL

In order to investigate the influence of the heat treatment process on the properties of hydroxyapatite powder; batches of hydroxyapatite powder (each one representing 250 g) were subjected to heat treatment at various temperatures. The batch was placed in a porcelain pot and inserted in a muffle furnace (Nobertherm program controller C19, Germany). Different calcination temperatures were applied ranged from 800 to 1100 °C with 100 °C intervals with a heating rate of 5 °C. After heat treatment the powder were kept in desiccators for the subsequent characterizations.

X-ray diffraction (XRD, Bruker axs D8, Karlsruhe, Germany) with $CuK_\alpha$ ($\lambda$ = 1.5406 Å) radiation and secondary monochromator was used to identify the type of phases, determine the crystallite size and the degree of crystallinity of the as received hydroxyapatite powder. The range of scans was $4° \leq 2\theta \leq 70°$ for crystalline phase identification and $25° \leq 2\theta \leq 26.3°$ for crystallite size measurement. Scan step was $0.02\theta$ with a step time of 2s. The size of the crystallites responsible for the Bragg reflection of the (002) plane was determined using the well-known Sherrer relationship (eqn. 1):

$$D = \frac{k\lambda}{B \cos\theta} \quad (1)$$

where D is the crystallite diameter in Å, k the shape constant (about 0.9), $\lambda$ the wavelength in Å (1.5406), $\theta$ the Bragg angle in degrees and B the observed peak width at half-maximum peak height in rad.

On the other hand the crystallinity degree, corresponding to the fraction of crystalline phase present in the examined volume, was evaluated by the relation (eqn. 2):

$$B_{002}\sqrt[3]{X_C} = K \quad (2)$$

where $X_C$ is the degree of crystallinity, K is a constant found equal to 0.24 for a very large number of different hydroxyapatite powders and $B_{002}$ is FWHM (°) of reflection (002).

The functional group analysis was performed by fourier transform infrared spectroscopy (FT-IR). The measurements were carried out in the transmission mode in the mid-infrared range (4000-400 $cm^{-1}$) at the resolution of 4 $cm^{-1}$. The studies were performed using the instrument of JASCO 3600, Tokyo, Japan. For FT-IR measurements, KBr pellets containing the exact weighted amount of the substance examined were prepared.

Morphology of samples was examined using scanning electron microscope (JEOL-JSM-5410 Tokyo, Japan) equipped with EDX unit (England, Oxford, ANCK).

The particle size distribution and the mean particle size ($d_{50}$) were determined by the laser diffraction method (FRITSCH Model ANALYSETTE 22, Idar-Oberstein, Germany). One gram of the sample was suspended with 10 mL bi-distilled water and then the produced suspension (produced with hand shaking) was employed for measuring size analysis. The specific surface area ($S_{BET}$) of the powder was determined by BET method using a surface area analyzer (Autosorb-1, Quantachrome Instruments, USA).

A laser Zetameter 'Malvern Instruments Model Zetasizer 2000' was used for zeta potential measurements. A 0.1 g of sample was placed in 50 mL bi-distilled water with pH modifiers; having the ionic strength of $2 \times 10^{-2}$ M NaCl. The suspension was conditioned for 30 h during which the pH was adjusted. After shaking, the equilibrium pH was recorded. Then 10 mL of the suspension was transferred into a standard cell for zeta potential measurement. Suspension temperature was maintained at 25 °C. Zeta potential was measured as a function of pH ($HNO_3$ 1 M and NaOH 1 M were used to adjust the pH). Five measurements were taken and the average was reported as the measured zeta potential. The isoelectric point (IEP) was identified at the pH axis crossing point.

For viscosity measurements, 20 g of the solid sample was placed with the required concentration percentage of the surfactant (polymer) solutions (100 $cm^3$) in a 200 $cm^3$ volumetric flasks and shaken by a shaker (JANKE & KUNKEL Type V × 10, Germany). The pH was adjusted to the desired values using HCl and NaOH. Then the sample was transferred to the Viscometer Model Anton paar DV-3p, Austria. For viscosity measurement a constant shear rate of 250 $s^{-1}$ was applied. Three measurements were taken at each point and its average was represented as the measured viscosity for the sample.

In turbidity experiments, 0.1 g dry sample was placed with the required concentration of surfactant (polymer) solutions (50 $cm^3$) in a 100 $cm^3$ volumetric flasks and shaken by a shaker (JANKE & KUNKEL Type V × 10, Germany). The pH was adjusted to the desired values using HCl and NaOH. The solution was shaken for 30 h at controlled room temperature of 25 °C. Then, the samples were transferred to the turbidity Inst. Model HANNA Instruments, Sweden, range 0.000 to 1,000 BTU. The measurements were replicated for three times for each sample and the average was taken as a measured turbidity degree.

## RESULTS AND DISCUSSION

### Effect of calcination temperatures on the properties of calcined powder

**XRD analysis:** Fig. 1 shows the XRD patterns of the as received hydroxyapatite powder and the samples after calcining at various temperatures. The XRD peaks of all five

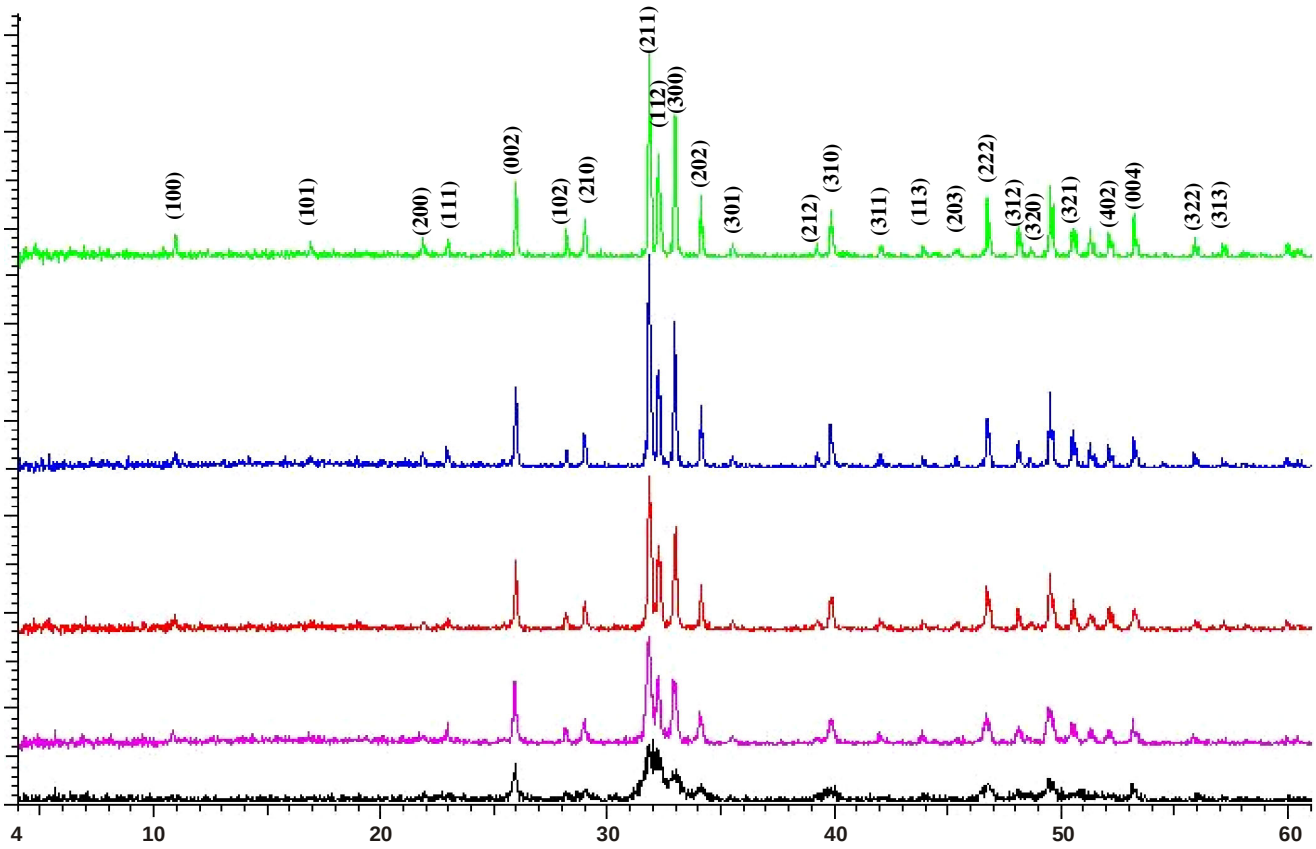


Fig. 1. XRD patterns of hydroxyapatite powder treated at different calcination temperatures

diffraction patterns are compared with that of standard hydroxyapatite in the powder diffraction file ((PDF card # 9-432). A good agreement between the experimental data (for all samples) and the standard hexagonal hydroxyapatite structure (PDF card # 9-432) both in term of intensity and d-spacing was obtained. Particularly the strong diffraction peaks corresponding to hydroxyapatite at 2θ position of 31.78 (211 plane) together with other two peaks at 32.266 (112 plane) and 32.951 (300 plane) confirmed that both as received powder and that calcined at various temperatures are pure hydroxyapatite of hexagonal structure[19]. However, no peaks were detected at 2θ of 29.4° and 39.93° which are characteristic peaks of calcium carbonate (calcite)[20] for both as received powder and that calcined at various temperatures. This confirmed that the different calcination temperatures not influenced the composition of the hydroxyapatite structure of the as received sample. On the other hand, no extraneous phases were detected in the examined 2θ range either before or after heat treatment.

Although the as received powder is composed of a pure hydroxyapatite it is clear from the XRD-pattern that it is present in poorly crystalline phase together with amorphous phase. Also the clear overlapping of the (211) and (112) peaks at 2θ–32 is clearly noticeable. This overlapping is an indication for the presence of hydroxyapatite phase in carbonated form[21]. As the calcination temperature is increased from 800 to 1100 °C, several hydroxyapatite lines become more distinct (especially at higher calcination temperature) which an indication of increasing the crystallinity degree. Also the width of the lines becomes narrower, which suggest an increasing in the crystalline size with increasing the calcination temperature.

Accordingly, both crystallinity degree and crystalline size variation with calcination temperature were evaluated using the XRD pattern with the aid of simple equations.

For the degree of crystallinity measurements, the equation of Landi *et al.*[22] was applied (eqn. 2). Whereas, the full width under half maximum for the (002) planes for samples treated at various calcination temperatures is given in Fig. 2.

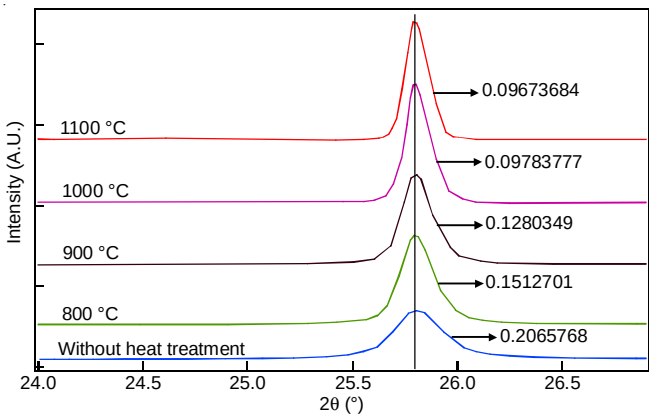


Fig. 2. FWHM for the (002) plane of hydroxyapatite at different calcination temperatures

Based on equation (2), the variation in the degree of crystallinity of hydroxyapatite sample with different calcination temperatures was calculated and given in Fig. 3. It was pointed

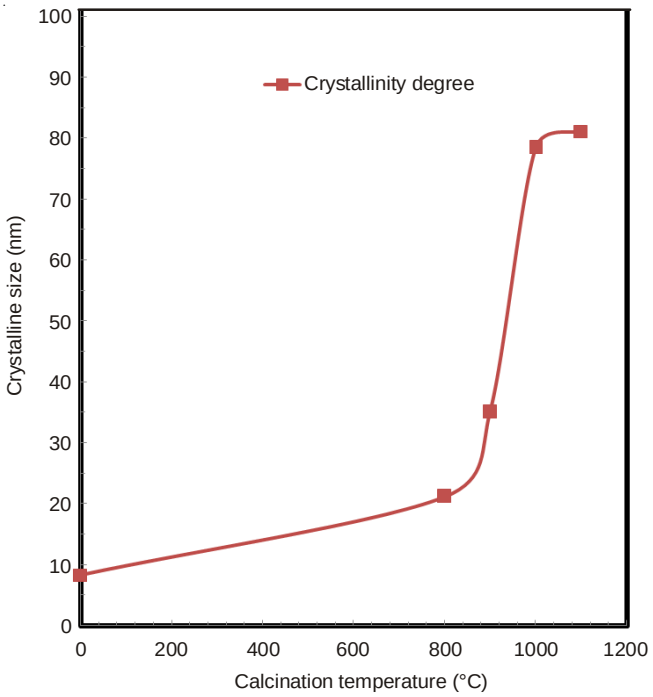


Fig. 3. Effect of calcination temperatures on the crystallinity degree of hydroxyapatite samples

out that the crystallinity degree is largely increased from 8 to 78 % with increasing calcination temperature from as received sample to 1000 °C, respectively. While beyond 1000 °C a slight increase in the crystallinity degree was observed at 1100 °C. The similar phenomenon was recorded by various authors[23-26].

On the other hand, the line broadening of (002), (211), (300), (202), (310), (222) and (213) reflections was used to evaluate the mean crystalline size of hydroxyapatite samples using Scherrer relationship (eqn. 2).

The variation in crystalline size of hydroxyapatite samples with different calcination temperatures was calculated and presented in Fig. 4. It was noticed that the crystalline size of hydroxyapatite samples was increased from 28 nm for as received powder to 190 nm for powder calcined at 1100 °C. The increase in crystalline size is found to follow two distinct steps. One of the as received powder to powder calcined at 800 °C, where the increase in crystalline size is slow from 28 nm to 65 nm, respectively. The other, in the high calcination temperatures ranges from 800 to 1100 °C where the size is increased rapidly from 65 to 190 nm, respectively. The slow growth rate in the first part may be ascribed to the crystallization of a large number of particles (confirmed from the low crystallinity degree of the as received powder with the occurrence of amorphous phase structure). In this stage crystallization is the predominant mechanism. In the second part growth of the crystallized particles takes place at a rapid rate with a diffusion controlled mechanism beside crystallization of other particles. The diffusion controlled coarsening of the powder on heating leads to grain growth of the crystallized particles results in increasing the crystalline size[27]. However, beyond 800 °C the two mechanisms (crystallization and diffusion) are simultaneously occurring at a high rate. Figs. 3 and 4 indicate that beyond 800 °C a rapid increase in both crystallinity degree and crystalline size is occurring. This

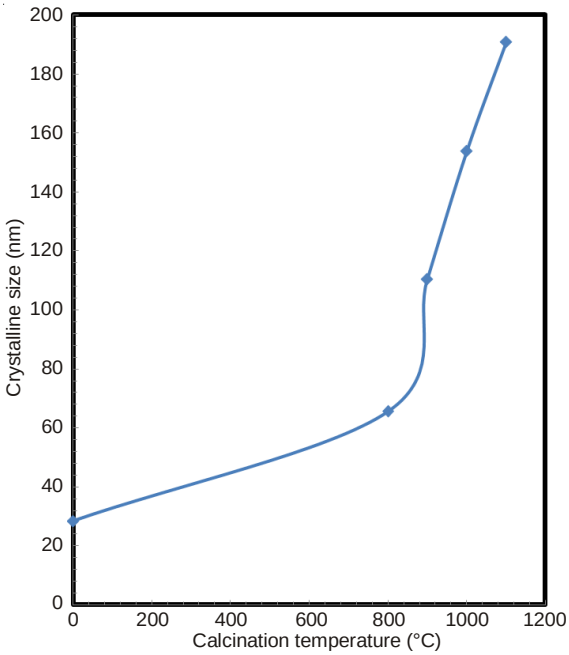


Fig. 4. Effect of different calcination temperatures on the crystalline size of hydroxyapatite samples

observation is rather confirmed from the SEM analysis of as received powder and powder calcined at various temperatures as showed in Fig. 5. These figures revealed that a large enhancement in grain growth was clearly noticed with increasing calcination temperatures.

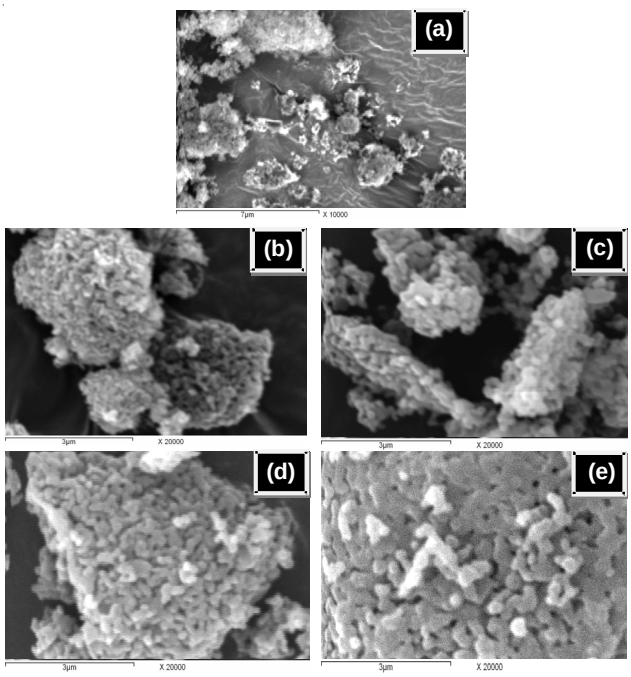


Fig. 5. SEM micrographs for hydroxyapatite powder calcined at various temperatures; (a) As received, (b) 800 °C, (c) 900 °C, (d) 1000 °C, and (e) 1100 °C

**FT-IR analysis:** To study the evolution of functional groups in the as received hydroxyapatite powder sample and that calcined at different temperatures, the FT-IR of these samples were analyzed. Functional groups that normally observed in the FT-IR of calcium phosphate based materials

are $PO_4^{3-}$, $OH^-$, $HPO_4^{2-}$ and $CO_3$ in the range[28] of 4000-300 $cm^{-1}$. There are four modes of $PO_4^{3-}$; $\nu_1$, $\nu_2$, $\nu_3$ and $\nu_4$ which gives bands at around 958, 500-400, 1100-1019 and 605-530 $cm^{-1}$, respectively[28]. On the other hand, there are three modes of $OH^-$ ions; stretching, vibration and translation, which give bands at 3700-2500, 630 and 390 $cm^{-1}$, respectively[29]. The $HPO_4^{2-}$ ions are observed at 875 $cm^{-1}$ band. However, overtone and combination of $\nu_3$ and $\nu_1$ modes of $PO_4^{3-}$ or even $HPO_4^{2-}$ appear in the 2200-1950 $cm^{-1}$ region[29,30]. Water molecules appear at 1642 $cm^{-1}$ but may be obscured by the $CO_3^{-2}$ band[30,31].

The $CO_3^{2-}$ ions, which replace $PO_4^{3-}$ ions in the hydroxyapatite lattice (designated as "B-type" carbonate) appear at about 1410 and 1450 $cm^{-1}$. While the $CO_3^{-2}$ that are supposed to replace $OH^-$ ions in the hydroxyapatite lattice (designated as "A-type" carbonate) gives bands[32] at 1455 and 1540 $cm^{-1}$.

Fig. 6 shows the FT-IR spectra of both as received hydroxyapatite powder and sample calcined at various temperatures. The band position and their respective assignments are given in Table-1. Fig. 6 and Table-1 revealed that there are some common features of the spectra produced from various samples. Whereas, there are many differences between these spectra are clearly noticeable.

The common features between the five spectra of different samples (as received and calcined at different temperatures) are:

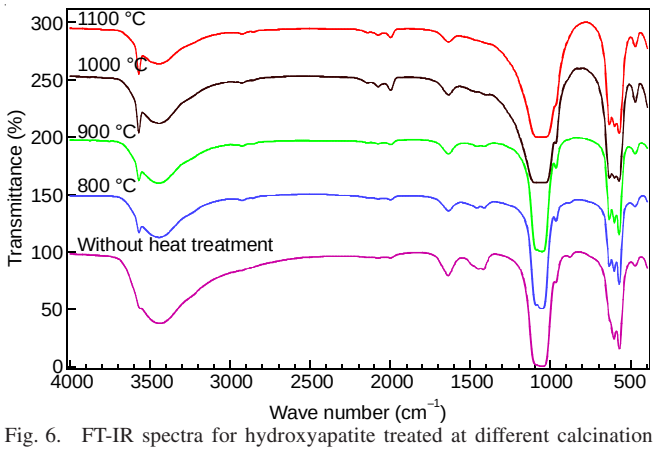


Fig. 6. FT-IR spectra for hydroxyapatite treated at different calcination temperatures

1. Appearance of absorption bands in the range of 1045, 964, 635 and 570 $cm^{-1}$ are characteristic bands of crystallized apatite phase[6].

2. All vibration modes of $PO_4^{3-}$ ($\nu_1$, $\nu_2$, $\nu_3$ and $\nu_4$) are clearly identified in all spectra. Bands appeared at ~964, 470, 1045-1095 and 570-605 $cm^{-1}$ are characteristic bands for $\nu_1$, $\nu_2$, $\nu_3$ and $\nu_4$ starching modes of $PO_4^{3-}$ ions, respectively.

3. Bands at 3444 and 1635 $cm^{-1}$ are relevant to the bending modes of hydroxyl groups in the absorbed water. While bands at 3571 $cm^{-1}$ as well as 633 $cm^{-1}$ (not observed only in the as received powder) are assigned to the stretching vibration of hydroxyl groups in the crystal structure of hydroxyapatite[34-37].

However, there are many differences between the spectrum of the as received hydroxyapatite sample and that calcined at various temperatures. These differences are pronounced in the appearance of new peaks with decreasing the intensities or even disappearance of the others. The followings are the main differences between the spectra that are noticeable from Fig. 6.

In the spectrum of as received hydroxyapatite, bands of $CO_3^{2-}$ was clearly detected in the region around 1460, 1416, 875 $cm^{-1}$. The band at 875 $cm^{-1}$ indicates the $\nu_2$ mode of $CO_3^{2-}$ group[38]. While, Mones *et al.*[39] and Xu *et al.*[33] have ascribed the appearance of bands at 872, 1417, 1460 $cm^{-1}$ for the presence of B-carbonated hydroxyapatite in which some of the $CO_3^{2-}$ ions substitute the $PO_4^{3-}$ ions in the hydroxyapatite structure. On the other hand, the XRD diffraction pattern of this sample (Fig. 1) not reveals any peaks characteristics for the presence of such compound (carbonated hydroxyapatite). This could attribute to the fact that, the strongest reflections of this compound arising from the (112) plane is lying at 2θ of 32.199, which almost overlaps with the 60 % relative intensity reflection of hydroxyapatite arising from (112) plane that lies at 2θ of 32.169. In addition, the lack of other peaks corresponding to the carbonated hydroxyapatite in the XRD of as received sample may be due to incomplete crystallization of this phase. This interpretation is consistent with a crystallinity degree calculation for such sample which revealed that this sample is nearly amorphous. By increasing the calcination temperatures a sharp decrease in the intensities of these bands

TABLE-1
FT-IR BAND ($cm^{-1}$) AND THEIR ASSIGNMENTS

| As received HA | Calcined hydroxyapatite | | | | Corresponding assignment |
|---|---|---|---|---|---|
| | 800 °C | 900 °C | 1000 °C | 1100 °C | |
| 3563.8 | 3571.5 | 3571.5 | 3571.5 | 3571.5 | OH- Stretching |
| 3440.4 | 3444.2 | 3444.2 | 3444.2 | 3444.24 | Absorbed $H_2O$ |
| - | - | 2144.5 | 2144.5 | 2140.6 | |
| 2078.9 | 2075 | 2075 | 2075 | 2075 | Combination of $\nu_1$ and $\nu_3$ modes of $PO_4^{3-}$ |
| 2001.7 | 1998 | 1998 | 1998 | 1998 | |
| 1635.3 | 1635.3 | 1635.3 | 1635.3 | 1635.3 | Water or $CO_3^{2-}$ |
| 1450.2 | 1458 | 1458 | 1458 | - | $CO_3^{2-}$ |
| 1419.4 | 1416 | 1411.6 | 1400 | - | |
| 1095.4 | 1091.5 | 1091.5 | 1091 | 1091 | $\nu_3$ mode of $PO_4^{3-}$ |
| 1045.2 | 1049.1 | 1052.9 | 1049 | 1045 | |
| 964.2 | 964.2 | 964.2 | 964.2 | 964.2 | $\nu_1$ mode of $PO_4^{3-}$ |
| 875.5 | 879.4 | 879 | 879 | - | $CO_3^{2-}$ |
| - | 632.5 | 632 | 632.5 | 632.5 | $OH^-$ Stretching |
| 605.5 | 601.7 | 601.7 | 601.7 | 601.7 | $\nu_4$ mode of $PO_4^{3-}$ |
| 570.83 | 570.83 | 570.83 | 570.8 | 570.8 | |
| 470.55 | 474.4 | 470.5 | 470.5 | 470.5 | $\nu_2$ mode of $PO_4^{3-}$ |

(corresponding to $CO_3^{-2}$) is detected. This indicates the elimination of $CO_3^{2-}$ due to the release of volatile gas with increasing temperature. However, the spectra indicate that these bands are almost disappearing for the sample calcined at 1000 °C while it completely disappears for sample calcined at 1100 °C. This indicates that samples calcined at both 1000 and 1100 °C are composed of crystallized hydroxyapatite without the presence of any of carbonated hydroxyapatite.

In the calcined samples, a new peak at 632.5 $cm^{-1}$ (which not observed in the as received sample) is clearly detected. This band is assigned to the stretching mode of $OH^-$ ion, which an indication of the presence of structural $OH^-$. The presence of this band in the spectra of calcined samples confirming the formation of characteristic apatite structure[12] and is indicative for the good crystallinity of hydroxyapatite sample[19]. This result is in good agreement with XRD data which revealed that the crystallinity degree is largely increased with increasing calcination temperatures.

The bands observed at 1635.3 and 3444 $cm^{-1}$ are assigned for the absorbed $H_2O$ which is quite usual to present in all hydroxyapatite samples. A high decrease in the intensities of these bands is clearly visible with increasing calcination temperatures. This is an indication of the loss of $H_2O$ molecules during calcination[19].

It could be easily noticed that the intensity of the peak appears at 3571 $cm^{-1}$ for as received sample is largely increased with increasing calcination temperatures and also become much sharper. This band is assigned to the OH stretching vibration mode and it is characteristic of apatite structure. Increasing the intensity of this band with the appearance of new bands in the range of 1900-2200 $cm^{-1}$ [assigned to ($\nu_1$ and $\nu_3$ modes of $PO_4^{3-}$ ion][40] is an evidence for increasing the crystallinity degree of hydroxyapatite sample with increasing calcination temperature.

**Particle size and surface area:** The effect of different calcination temperatures on the particle size and its distribution of hydroxyapatite powder were shown in Fig. 7. The mean particle size was found to increase from 3.4 μm for the as received sample to 16.9 μm for sample calcined at 1100 °C. Fig. 8 shows the variation in the mean particle size of hydroxyapatite samples calcined at different temperatures. However, there was no phase transformation was detected in the XRD pattern (Fig. 1). This means that the increase in the mean particle size is mainly the result of the necking of particles during the calcination process[10] which favor a grain growth of hydroxyapatite particles as previously described in the reason of increasing the crystalline size with calcination temperature. Increasing the calcination temperature gives the system adequate kinetics to permit further growth of hydroxyapatite grains[24].

The grain growth of hydroxyapatite particles with temperature can be ascribed by nucleation-aggregation-agglomeration growth mechanism[41]. According to this mechanism, hydroxyapatite particle growth through three steps: (a) nucleation and growth to form hydroxyapatite nanocrystallites, (b) aggregation of elemental nanocrystals by molecular attraction[42] of different nanometric/colloidal scale forces which cause surface free energy minimization, c) further crystal growth, at a constant residual super-saturation, acting as a cementing

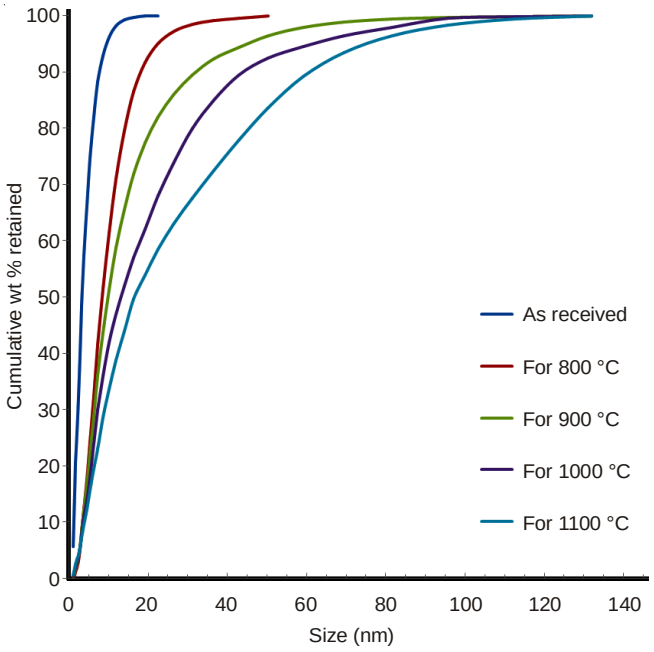


Fig. 7. Cumulative weight retained for hydroxyapatite powder treated at different calcination temperatures

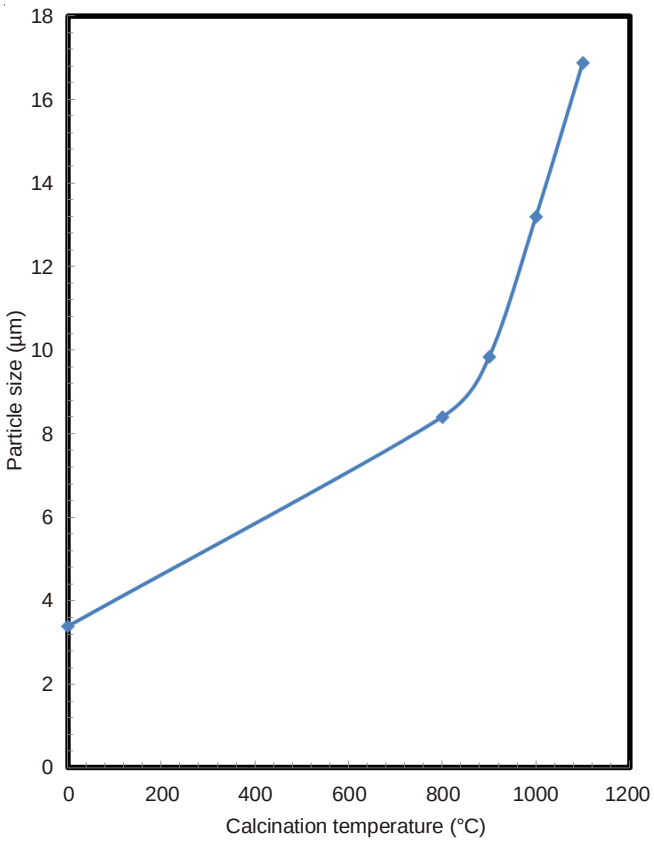


Fig. 8. Effect of calcination temperatures on the mean particle size of calcined samples

agent inside the aggregate to form agglomerates. The increase in particle size with temperature takes place by the aggregation of these agglomerated particles to form large particle. On the other hand, this mechanism of grain growth with temperature could be confirmed from the increasing of crystalline size with temperature as deduced from Fig. 4.

Fig. 9 shows the adsorption isotherm of the as received and calcined samples, while the specific surface area of different samples is given in Table-2. It was found that, the as received hydroxyapatite sample has the highest value of specific surface area of 74 $m^2/g$ while it is largely decreased for calcined samples. The specific surface area of calcined powders was found to be about 20, 10, 5 and 2 $m^2/g$ for sample calcined at 800, 900, 1000 and 1100 °C, respectively. The decrease in specific surface area with increasing calcination temperature was attributed to the increase in the particle size of hydroxyapatite powder upon calcination[21,43].

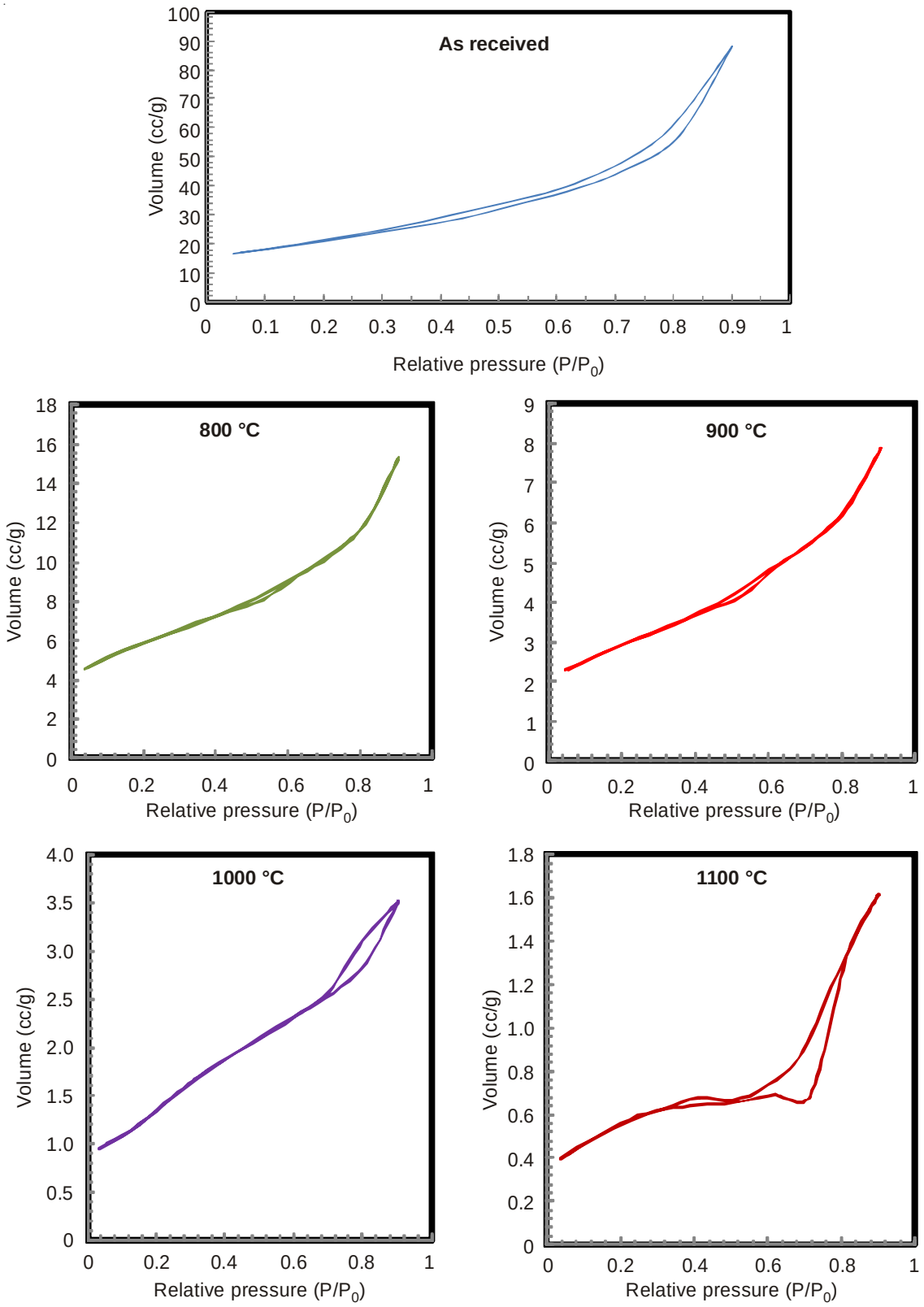


Fig. 9. Adsorption-Desorption isotherm for hydroxyapatite powder treated at different calcination temperatures

On the other hand, the pore volume as well as the pore size distribution of hydroxyapatite powder as a function of calcination temperatures are shown in Figs. 10 and 11, respectively. It was found that the pore volume is largely decreased with increasing calcination temperatures, while it is approximately eliminated when the powder is calcined at 1100 °C. However, the pore size distribution confirmed that all powders have a wide pore size distribution started from mesoporous range 2-50 nm to macroporous region > 50 nm. It is also confirmed that the overall porosity degree is largely reduced with increasing temperature and even eliminated when the calcination temperatures reached 1100 °C. This parameter is very important when dealing with preparation of well stabilized colloidal suspensions from hydroxyapatite powder. Because beside chemical composition and surface area of the powder, pore volume and its distribution is another factor which is largely influenced the suspensions fluidity. For powder having high pore volume a part of the liquid in a suspension is immobilized inside the pores. Therefore the effective volume of liquid would be higher with utilization of lower porosity powder[9]. Accordingly decreasing the pore volume and its distribution of the powder will enhance to a large extent the stability of the suspensions produced from it.

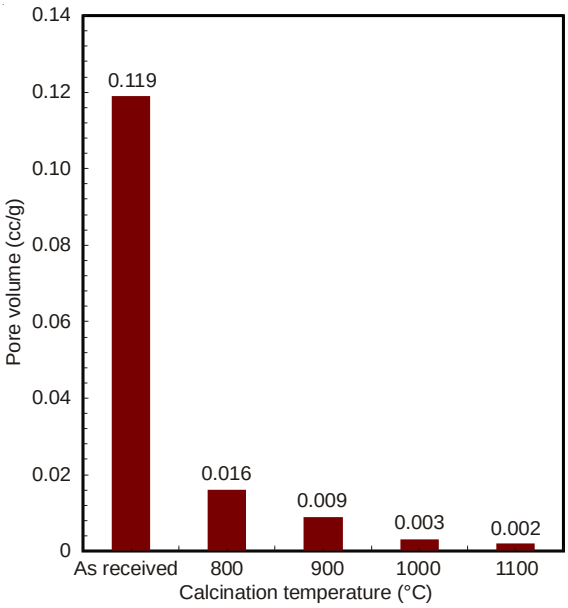


Fig. 10. Effect of calcination temperatures on the pore volume of hydroxyapatite powder

**Effect of calcination temperatures on zeta potential of powder:** It is well known that the surface properties of hydroxyapatite particles are very much sensitive to the history of the powder processing route as well as the heat treatment process[44]. The heat treatment process was found to be an important step in achieving a sufficient surface charge and a high zeta potential value which is a prerequisite for the preparation of a suspension with a sufficiently high solid loading[8,43-45].

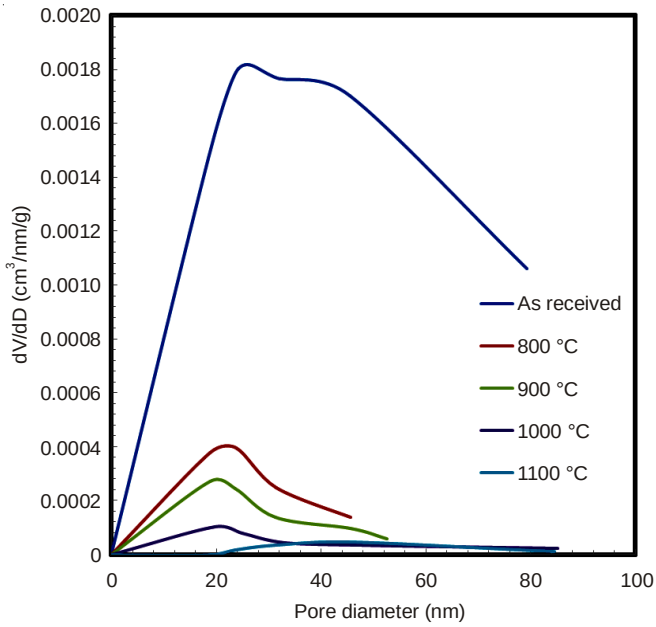


Fig. 11. Effect of calcination temperatures on the pore size distribution of hydroxyapatite powder

Fig. 12 shows the zeta potential as a function of pH for as received hydroxyapatite sample as well as samples calcined at various temperatures. The deviation of isoelectric point to a more acidic region with increasing calcination temperatures are clearly noticeable. This behaviour could attribute to the presence of the carbonate group in the as received hydroxyapatite powder. The presence of this group changes the surface behaviour of the powder making a shift for the isoelectric point (iep) to a higher basic region[21]. With increasing calcination temperatures the quantity of carbonate ions in calcined samples is largely decreased till it completely eliminated at the 1100 °C (as confirmed from the FT-IR data shown in Fig. 6), which interpret the shifting in the (iep) of these powders to more acidic region. However, it could also notice that by increasing the pH value, more negative charge established on the surface of hydroxyapatite particles for both as received and calcined samples. The highest negative charges was attained at pH of ~11 at which zeta potentials were found to be ~ -29, ~ -20, ~ -9, ~ -8 and ~ -3 for sample calcined at 1100, 1000, 900, 800 °C and as received, respectively. The highest negative charge was achieved for sample calcined at 1100 °C. Accordingly, this sample was chosen for investigate the effect of dispersing agent amounts and types on both viscosity and turbidity of suspensions prepared from it.

**Effect of type and amount of dispersing agent on zeta potential:** When hydroxyapatite particles dispersed into aqueous to overcome it might have various ions on their surfaces (such as $Ca^{2+}$, $CaOH^{+}$, $PO_4^{3-}$, $HPO_4^{2-}$, $H_2PO_4^{-}$ and $CaH_2PO_4^{+}$). Accordingly, hydroxyapatite suspension can be stabilized by using of anionic polyelectrolyte[46]. The study on the effect of calcination

TABLE-2
EFFECT OF CALCINATION TEMPERATURES ON THE SURFACE AREA OF HYDROXYAPATITE SAMPLES

| Sample type | As received HA | Calcined HA | | | |
|---|---|---|---|---|---|
| | | 800 °C | 900 °C | 1000 °C | 1100 °C |
| Surface area ($m^2/g$) | 73.867 | 20.026 | 10.091 | 5.157 | 1.895 |

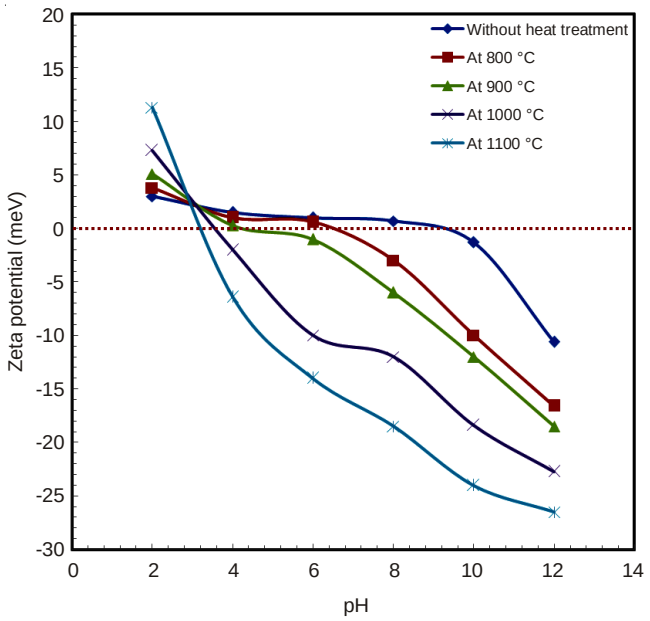


Fig. 12. Zeta potential – pH relationship of hydroxyapatite powder treated at different calcination temperatures

temperatures on zeta potential of hydroxyapatite particles revealed that these particles are thermodynamically stable in the alkaline pH region. It is recognized that the anionic type dispersants help to develop high zeta potentials in the neutral or alkaline pH regions and are more effective in stabilizing hydroxyapatite suspensions than non-ionic dispersant[47]. These anionic polyelectrolyte modify the surface chemistry of powder in order to produce repulsive inter-particle forces that promote dispersion. Polyacrylate dispersant (represent a large group of anionic polyelectrolyte) proved to be effective dispersing agents for both clay and non-clay based ceramics, through an electrosteric mechanism of dispersing action. The combination of electrostatic and steric stabilization mechanisms (electrosteric mechanism) is important, especially in case of high solids concentration where the average inter-particle distance is short[48,49]. Accordingly, two types of polyacrylate dispersants namely poly acrylic acid (PAA) and sodium poly acrylate (SPA) were applied to further investigations for stabilizing hydroxyapatite suspension.

The zeta potential - pH curves for hydroxyapatite powder calcined at 1100 °C with various concentrations of both poly acrylic acid and sodium poly acrylate was shown in Fig. 13. It revealed that increasing both pH and concentration of dispersing agent are responsible for increasing the particle surface charge. However, it was found that sodium poly acrylate develop much higher negative charge on the hydroxyapatite particles than done by the using of poly acrylic acid dispersant. This means that sodium poly acrylate could be much powerful dispersant for stabilizing hydroxyapatite suspension than poly acrylic acid. In addition the differences in zeta potential values is not so large between the two types of dispersant. In order to decide whether sodium poly acrylate or poly acrylic acid is much powerful in stabilizing hydroxyapatite suspension a study for the viscosity and turbidity of these suspensions with the addition of different concentration of both dispersant should be investigated. Also, it could be noticed that at pH 11 a higher negative charge for hydroxyapatite particles was obtained whatever the calcination temperature as well as the type and amount of dispersants.

**Effect of type and amount of dispersing agent on viscosity and turbidity of hydroxyapatite suspension:** A 20 wt. % suspensions from hydroxyapatite powder calcined at 1100 °C were prepared for performing both viscosity and turbidity measurements.

Figs. 14 A and B show the effect of both type and amount of dispersant on the viscosity of suspensions prepared from powder calcined at 1100 °C. It was noticed that with increasing time the viscosity of all suspensions is largely decreased. This is an indication of the shear thinning behaviour of such suspensions. On the other hand, it was noticed that a minimum viscosity was observed at 0.36 wt. % of both dispersant additions. This observation revealed that the 0.36 wt. % of dispersant correlate with the optimum concentration for complete coverage of dispersant on ceramic particles creating a maximum repulsive potential, resulting in a low viscosity suspension[50]. At this amount of dispersant the system is reached what's called saturation absorption point. At this point the dissociated sodium poly acrylate and poly acrylic acid may cover the surface of all hydroxyapatite particles and these particles would behave a mono-dispersed particle due to electrosteric stabilization resulting in obtaining a lower viscosity hydroxyapatite suspension. At the lower amount addition of dispersant (0.24 wt. %) a non-complete coverage of hydroxyapatite particles is obtained, consequently the produced electrical double layer

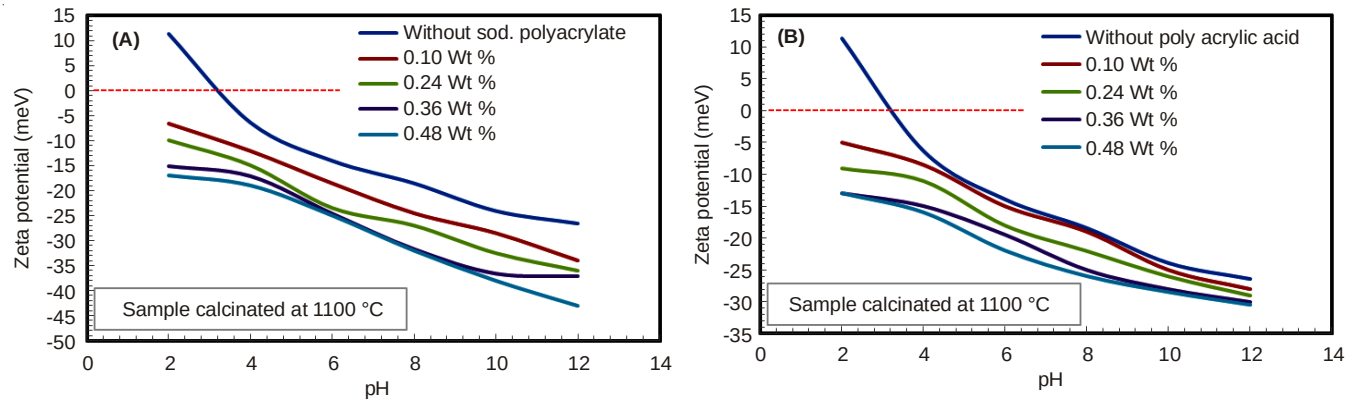


Fig. 13. Zeta potential - pH relationship of hydroxyapatite powder with different weight percentage addition of various dispersing agents; (A) = Sod. poly acrylate; (B) = Poly acrylic acid

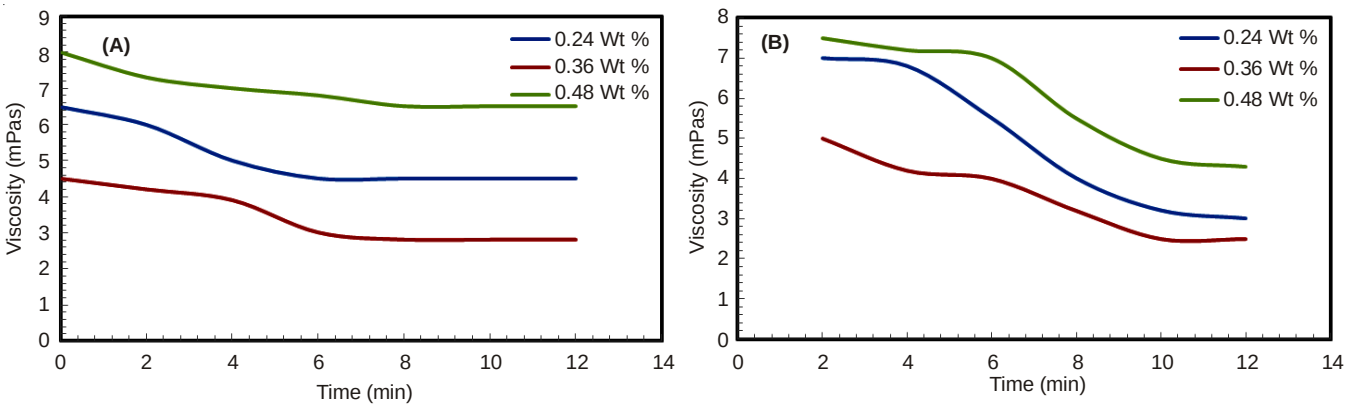


Fig. 14. Viscosity of 20 % solid loading hydroxyapatite powder with different weight percentage addition of various dispersing agents; A = Sod. poly acrylate; B = Poly acrylic acid

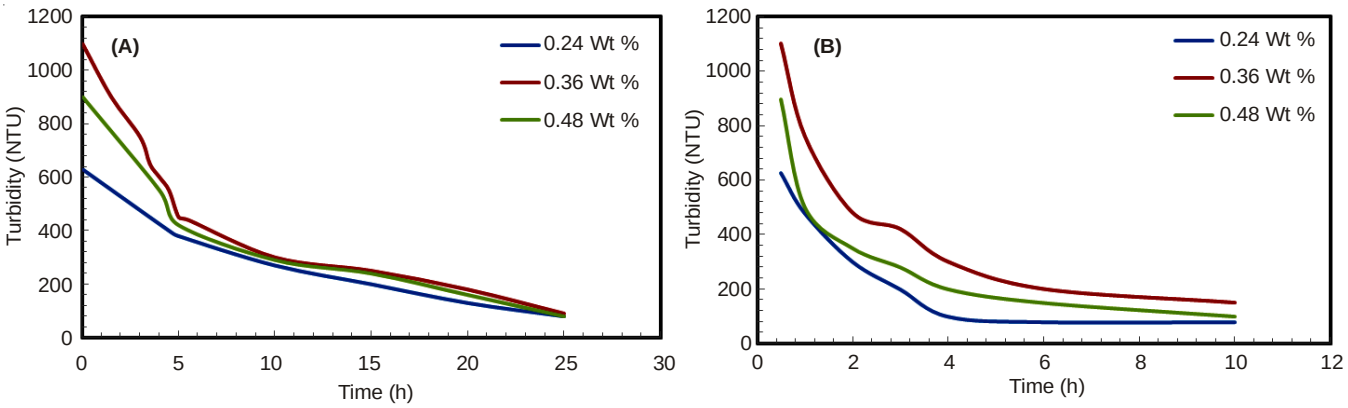


Fig. 15. Turbidity measurement of hydroxyapatite powder with different weight percentage addition of various dispersing agents; A = Sod. poly acrylate; B = Poly acrylic acid

is not enough to achieve an effective inter-particles repulsion and prevails the attraction between them[21]. When the amount of dispersant is higher than the saturated absorption point, the free polyelectrolyte would exist in the aqueous medium. This cause the electrical double layer to be compressed by too high electrolyte concentration and makes the electrostatic repulsion less effective and consequently the viscosity increased[21]. Also the increase in the amount of dispersant may cause interlocking of polyelectrolyte chain, which bridged the solid particles and caused increased the suspension viscosity[25].

This previous phenomenon of the presence of the optimum amount of dispersant for producing lowest hydroxyapatite suspension viscosity could be rather confirmed from the turbidity measurements shown in Fig. 15. Figs. 15 A, B show that the turbidity degree is higher with the addition of 0.36 wt. % of both dispersant. Increasing the amount of dispersant than this value leads to a high decrease in the degree of turbidity. This observation rather confirmed the interpretation of the presence of the optimum amount of dispersant in order to achieve a lowest hydroxyapatite suspension viscosity.

## Conclusion

In conclusion, the heat treatment step plays a very important role in controlling the various physical as well as chemical properties of hydroxyapatite powder. A well crystallized hydroxyapatite powder was achieved with increasing the calcination temperature while both crystalline size and particle size is largely increased. The carbonate ion content is largely reduced with increasing the calcination temperature and it is almost eliminated when the calcination temperature reaches 1100 °C. Besides the high decrease in the specific surface area with calcination, the pore size and its distribution were found to be largely reduced with increasing calcination temperatures, which helps in the preparation of well stabilized hydroxyapatite suspension of high solid loading. Zeta potential measurements confirmed the development of high negative charge on hydroxyapatite particles calcined at high temperature. The effect of different types and amounts of two dispersant agents (polyacrylic acid and sodium polyacrylate) on zeta potential (for powder calcined at 1100 °C) revealed that sodium poly acrylate is much more effective in developing high zeta potential value on hydroxyapatite particles. Viscosity and turbidity measurements define that there is an optimum amount of dispersant agent for producing hydroxyapatite suspension of lower viscosity and high turbidity degree. The calcination temperature 1100 °C proves to be the most suitable calcination temperature for producing hydroxyapatite powder possesses reasonable physical properties for developing well stabilized hydroxyapatite suspension.

## ACKNOWLEDGEMENTS

The authors are thankful to the Science and Technology Development fund in Egypt, for funding this work under the project No. 806.

## REFERENCES


1. W. Cao and L.L. Hench, *Ceram. Int.*, **22**, 493 (1996).
2. G. Daculsi, *Biomaterials*, **19**, 1473 (1998).
3. S. Yamada, D. Heymann, J.M. Bouler and G. Daculsi, *J. Biomed. Mater. Res.*, **37**, 346 (1997).
4. K. de Groot, *Biomaterials*, **1**, 47 (1980).
5. W. Suchanek and M. Yoshimura, *J. Mater. Res.*, **13**, 94 (1998).
6. G. de With, H.J.A. van Dijk, N. Hattu and K. Prijs, *J. Mater. Sci.*, **16**, 1592 (1981).
7. H.Y. Yasuda, S. Mahara, Y. Umakoshi, S. Imazato and S. Ebisu, *Biomaterials*, **21**, 2045 (2000).
8. J. Zhang, M. Maeda, N. Kotobuki, M. Hirose, H. Ohgushi, D. Jiang and M. Iwasa, *Mater. Chem. Phys.*, **99**, 398 (2006).
9. S. Padilla, R. Garcia-Carrodeguas and M. Vallet-Regý, *J. Eur. Ceram. Soc.*, **24**, 2223 (2004).
10. H.Y. Juang and M.H. Hon, *Ceram. Int.*, **23**, 383 (1997).
11. Y.H. Koh, H.W. Kim, H.E. Kim and J.W. Halloran, *J. Am. Ceram. Soc.*, **85**, 2578 (2002).
12. Y. Zhang, Y. Yokogawa, X. Feng, Y. Tao and Y. Li, *Ceram. Int.*, **36**, 107 (2010).
13. C.Y. Tan, R. Tolouei, S. Ramesh, B.K. Yap and M. Amiriyan, *IFMBE Proc.*, **35**, 51 (2011).
14. N. Patel, I.R. Gibson, S. Ke, S.M. Best and W. Bonfield, *J. Mater. Sci.; Mater. Med.*, **12**, 181 (2001).
15. A. Sobczak-Kupiec, Z. Wzorek, R. Kijkowska and Z. Kowalski, *Bull. Mater. Sci.*, **36**, 755 (2013).
16. H.Y. Juang and M.H. Hon, *Biomaterials*, **17**, 2059 (1996).
17. M. Figueiredo, A. Fernando, G. Martins, J. Freitas, F. Judas and H. Figueiredo, *Ceram. Int.*, **36**, 2383 (2010).
18. J.A. Toque, M.K. Herliansyah, M. Hamdi, A. Ide-Ektessabi and M.W. Wildan, *IFMBE Proc.*, **15**, 152 (2007).
19. S. Ahmed and M. Ahsan, *J. Sci. Ind. Res. (India)*, **43**, 501 (2008).
20. U. Vijayalakshmi and S. Rajeswari, *Trends Biomater.Artif. Organs*, **19**, 57 (2006).
21. E. Landi, G. Celotti, G. Logroscino and A. Tampieri, *J. Eur. Ceram. Soc.*, **23**, 2931 (2003).
22. E. Landi, A. Tampieri, G. Celotti and S. Sprio, *J. Eur. Ceram. Soc.*, **20**, 2377 (2000).
23. K.P. Sanosh, M.C. Chu, A. Balakrishnan, T.N. Kim and S.J. Cho, *Bull. Mater. Sci.*, **32**, 465 (2009).
24. J. Klinkaewnarong and S. Maensiri, *J. Sci.*, **37**, 243 (2010).
25. T. Tian, D. Jiang, J. Zhang and Q. Lin, *J. Eur. Ceram. Soc.*, **27**, 2671 (2007).
26. E. Bouyer, F. Gitzhofer and M.I. Boulos, *J. Mater. Sci. Mater. Med.*, **11**, 523 (2000).
27. Pratihar, M. Garg, S. Mehra and S. Bhattacharyya, *J. Mater. Sci. Mater. Med.*, **17**, 501 (2006).
28. A.S.F. Alqap and I. Sopyan, *Indian J. Chem.*, **48A**, 1492 (2009).
29. I. Mobasherpour, M.S. Heshajin, A. Kazemzadeh and M. Zakeri, *J. Alloys Comp.*, **430**, 330 (2007).
30. S. Bose and S.K. Saha, *Chem. Mater.*, **15**, 4464 (2003).
31. G. Guo, Y. Sun, Z. Wang and H. Guo, *Ceram. Int.*, **31**, 869 (2005).
32. K. Donadel, M.C.M. Laranjeira, V.L. Goncalves, V.T. Favere, J.C. De Lima and L.H. Prates, *J. Am. Ceram. Soc.*, **88**, 2230 (2005).
33. G. Xu, I.A. Aksay and J.T. Groves, *J. Am. Chem. Soc.*, **123**, 2196 (2001).
34. K. Lin, J. Chang, R. Cheng and M. Ruan, *Mater. Lett.*, **61**, 1683 (2007).
35. Y. Sun, G. Guo, Z. Wang and H. Guo, *Ceram. Int.*, **32**, 951 (2006).
36. G. Felício-Fernandes and M.C.M. Laranjeira, *Quim. Nova*, **23**, 441 (2000).
37. I. Sopyan, R. Singh and M. Hamdi, *Indian J. Chem.*, **47A**, 1626 (2008).
38. J.C. Elliott, Structure and Chemistry of the Apatites and Other Calcium Orthophosphates, Amsterdam: Elsevier, pp. 387 (1994).
39. P. Moens, F. Callens, P. Matthys, F. Maes, R. Verbeeck and D. Naessens, *J. Chem. Soc., Faraday Trans.*, **87**, 3137 (1991).
40. I.R. Gibson, I. Rehman, S.M. Best and W. Bonfield, *J. Mater. Sci. Mater. Med.*, **11**, 533 (2000).
41. A.D. Randolph and M.A. Larson, Theory of Particulate Processes, Academic Press, New York, edn 2, pp. 369 (1986).
42. J. Gomez-Morales, J. Torrent-Burgues and R. Rodriguez-Clemente, *Cryst. Res. Technol.*, **36**, 1065 (2001).
43. M.R. Saeri, A. Afshar, M. Ghorbani, N. Ehsani and C.C. Sorrell, *Mater. Lett.*, **57**, 4064 (2003).
44. S. Bhattacharjee, S.K. Swain, D.K. Sengupta and B.P. Singh, *Colloids Surf. A*, **277**, 164 (2006).
45. Z. Sadeghian, J.G. Heinrich and F. Moztarzadeh, *Ceram. Int.*, **32**, 331 (2006).
46. T. Navizi, E. Salahi, M. Ghafari and I. Mobasherpour, *Ceram. Int.*, **36**, 1945 (2010).
47. F. Lelievre, D. Bernach-Assollant and T. Chartier, *J. Mater. Sci. Mater. Med.*, **7**, 489 (1996).
48. A.B. Corradi, T. Manfredini, G.C. Pellacani and P. Pozzi, *J. Am. Ceram. Soc.*, **77**, 509 (1994).
49. S. Baklouti, C. Pagnoux, T. Chartier and J.F. Baumard, *J. Eur. Ceram. Soc.*, **17**, 1387 (1997).
50. L.A. Cyster, D.M. Grant, S.M. Howdle, F.R.A.J. Rose, D.J. Irvine, D. Freeman, C.A. Scotchford and K.M. Shakesheff, *Biomaterials*, **26**, 697 (2005).